



Heterozygous mutations of the kinesin *KIF21A* in congenital fibrosis of the extraocular muscles type 1 (CFEOM1)

Koki Yamada^{1,2}, Caroline Andrews^{1,2}, Wai-Man Chan¹, Craig A McKeown³, Adriano Magli⁴, Teresa de Berardinis⁴, Anat Loewenstein⁵, Moshe Lazar⁵, Michael O'Keefe⁶, Robert Letson⁷, Arnold London⁸, Mark Ruttum⁹, Naomichi Matsumoto¹⁰, Nakamichi Saito¹¹, Lisa Morris¹², Monte Del Monte¹², Roger H Johnson¹³, Eiichiro Uyama¹⁴, Willem A Houtman¹⁵, Berendina de Vries¹⁵, Thomas J Carlow¹⁶, Blaine L Hart¹⁶, Nicolas Krawiecki¹⁷, John Shoffner¹⁸, Marlene C Vogel¹⁹, James Katowitz²⁰, Scott M Goldstein²⁰, Alex V Levin²¹, Emin C Sener²², Banu T Ozturk²², A Nurten Akarsu²³, Michael C Brodsky²⁴, Frank Hanisch²⁵, Robert P Cruse²⁶, Alina A Zubcov²⁷, Richard M Robb²⁸, Peter Roggenkämper²⁹, Irene Gottlob³⁰, Lionel Kowal³¹, Ravi Battu³², Elias I Traboulsi³³, Piergiorgio Franceschini³⁴, Anna Newlin³⁵, Joseph L Demer³⁶, Elizabeth C Engle^{1,2,37}

Congenital fibrosis of the extraocular muscles type 1 (CFEOM1; OMIM #135700) is an autosomal dominant strabismus disorder associated with defects of the oculomotor nerve. We show that individuals with CFEOM1 harbor heterozygous missense mutations in a kinesin motor protein encoded by *KIF21A*. We identified six different mutations in 44 of 45 probands. The primary mutational hotspots are in the stalk domain, highlighting an important new role for *KIF21A* and its stalk in the formation of the oculomotor axis.

CFEOM1 is associated with absence of the superior division of the oculomotor nerve and corresponding midbrain motoneurons and profound atrophy of the two muscles normally innervated by this nerve, the levator palpebrae superioris and superior rectus¹. These two muscles elevate the eyelid and the globe, and their dysfunction accounts for the primary features of the CFEOM1 phenotype^{2–4} (Fig. 1a).

We previously mapped CFEOM1 to a 2.1-cM interval at 12cen (*FEOM1* locus)^{2–5}. We screened the 17 published CFEOM1 pedigrees^{2–5} whose phenotypes map to *FEOM1* for mutations in transcripts from this region. After excluding several candidates, we examined two adjacent partial transcripts, *FLJ20052* and *KIAA1708*, that share similarity to mouse *Kif21a*⁶. Combining database sequence with that generated from human fetal brain cDNA by RT-PCR, we determined the cDNA and genomic organization of human *KIF21A*. The *KIF21A* open reading frame is 5,022 bp in length, comprises 38 exons with alternative splicing of exon 12 and exons 29–31, encompasses a genomic region of ~150 kb and is predicted to encode a protein of 1,674 amino acids (Fig. 1b; see **Supplementary Methods** online).

We examined the 38 *KIF21A* coding exons and flanking intronic sequence and identified heterozygous missense mutations in each of the 17 unrelated probands (Table 1a and Fig. 1c,d). Eleven probands harbored a 2,860C→T nucleotide substitution (resulting in the amino acid substitution R954W) and four probands harbored the substitution 2,861G→A (resulting in R954Q), located at the first and second nucleotide positions of codon 954, respectively. One proband harbored the substitution 3,029T→C (resulting in I1010T), 56 residues downstream of the two recurrent mutations. The remaining proband harbored the substitution 1,067T→C (resulting in M356T). To ensure that the 2,860C→T mutation in exon 21 and the 1,067T→C mutation in exon 8 did not disrupt splicing, we successfully amplified single amplicons of the correct size across exons 19–23 and 6–11 using template cDNA from immortalized lymphoblasts of an affected member of pedigrees BL and FH (data not shown).

¹Department of Medicine (Genetics), Enders 5, Children's Hospital Boston, 300 Longwood Avenue and ²Harvard Medical School, Boston, Massachusetts 02115, USA. ³Department of Ophthalmology, Bascom Palmer Eye Institute, Miami, Florida, USA. ⁴Università degli Studi di Napoli Dipartimento di Scienze Oftalmologiche, Naples, Italy. ⁵Department of Ophthalmology, Sackler Faculty of Medicine, Tel-Aviv University, Tel-Aviv, Israel. ⁶Department of Ophthalmology, The Children's Hospital, Dublin, Ireland. ⁷Department of Ophthalmology, University of Minnesota, St. Paul, Minnesota, USA. ⁸Department of Pediatrics, Aspen Medical Group, St. Paul, Minnesota, USA. ⁹Department of Ophthalmology, Medical College of Wisconsin, Milwaukee, Wisconsin, USA. ¹⁰Department of Human Genetics, Nagasaki University Graduate School of Biomedical Sciences, Nagasaki, Japan. ¹¹Department of Gynecology, Shin-Koga Hospital, Kurume, Japan. ¹²Kellogg Eye Center, University of Michigan, Ann Arbor, Michigan, USA. ¹³Department of Ophthalmology, Children's Hospital, University of Washington, Seattle, Washington, USA. ¹⁴Department of Neurology, Kumamoto University School of Medicine, Kumamoto, Japan. ¹⁵Department of Ophthalmology, University Medical Centre, Groningen, The Netherlands. ¹⁶Department of Radiology & Ophthalmology, University of New Mexico, Albuquerque, New Mexico, USA. ¹⁷Department of Pediatrics, Emory University School of Medicine, Atlanta, Georgia, USA. ¹⁸Horizon Molecular Medicine, Atlanta, Georgia, USA. ¹⁹Department of Ophthalmology, Hospital de Niños 'Roberto del Río', Santiago, Chile. ²⁰Department of Ophthalmology, Children's Hospital of Philadelphia, Philadelphia, Pennsylvania, USA. ²¹Department of Ophthalmology, The Hospital for Sick Children, Toronto, Ontario, Canada. ²²Departments of Ophthalmology and ²³Pediatrics, Hacettepe University Medical Faculty, Ankara, Turkey. ²⁴Departments of Ophthalmology & Pediatrics, University of Arkansas, Little Rock, Arkansas, USA. ²⁵Department of Neurology, Martin-Luther University Halle-Wittenberg, Halle, Germany. ²⁶Department of Pediatrics, Baylor College of Medicine, Houston, Texas, USA. ²⁷University Eye Hospital, Frankfurt, Germany. ²⁸Department of Ophthalmology, Children's Hospital Boston, Boston, Massachusetts, USA. ²⁹University Eye Clinic, Bonn, Germany. ³⁰Department of Ophthalmology, Leicester University, Leicester, UK. ³¹Department of Ophthalmology, University of Melbourne, Melbourne, Australia. ³²Department of Ophthalmology, St. John's Medical College, Bangalore, India. ³³Cole Eye Institute, Cleveland Clinic Foundation, Cleveland, Ohio, USA. ³⁴Centro Universitario di Dismorfologica Clinica, Università di Torino, Torino, Italy. ³⁵Department of Ophthalmology, University of Illinois, Chicago, Illinois, USA. ³⁶Departments of Ophthalmology and Neurology and the Jules Stein Eye Institute, University of California, Los Angeles, California, USA. ³⁷Department of Neurology, Children's Hospital Boston, Boston, Massachusetts, USA. Correspondence should be addressed to E.C.E (engle@enders.tch.harvard.edu).

Table 1 CFEOM1 probands and *KIF21A* mutation analysis

References	Pedigree	Origin	Mutated nt ^a	Altered aa	Exon	<i>De novo</i>	DAH ^b	
(a) Screening CFEOM1 pedigrees with published linkage data								
1–4	A	USA-MEA	2,860C→T	R954W	21		1	
2–4	B	Canada	2,860C→T	R954W	21		2	
3,4	C	Israel	2,860C→T	R954W	21		3	
4	T	Ireland	2,860C→T	R954W	21		4	
3,4	AA	USA-MEA	2,860C→T	R954W	21		1	
3,4	AD	USA-German	2,860C→T	R954W	21		5	
4	AG	USA	2,860C→T	R954W	21		6	
4	AJ	USA	2,860C→T	R954W	21		1	
4	BC	Japan	2,860C→T	R954W	21	Yes	7	
4	BJ	USA-British	2,860C→T	R954W	21		1	
4,13	CZ	Italy	2,860C→T	R954W	21		1	
4	E	Venezuela	2,861G→A	R954Q	21		18	
3,4	AC	USA-FC	2,861G→A	R954Q	21		19	
4	AH	USA	2,861G→A	R954Q	21		20	
4	CT	USA-MEA	2,861G→A	R954Q	21	Yes	21	
3,4	H	Netherlands	3,029T→C	I1010T	21		23	
5	FH	Japan	1,067T→C	M356T	8		25	
(b) New autosomal dominant CFEOM1 pedigrees								
	AI	USA-MEA	2,860C→T	R954W	21		8	
	AZ	Canada	2,860C→T	R954W	21		1	
	CD	USA-Hispanic	2,860C→T	R954W	21		9	
	CM	Turkey	2,860C→T	R954W	21		10	
	DL	Italy	2,860C→T	R954W	21	Yes	11	
14	EO	USA-MEA	2,860C→T	R954W	21	Yes	12	
15	EX	USA	2,860C→T	R954W	21		1	
	FB	Chile	2,860C→T	R954W	21		1	
	FD	Germany	2,860C→T	R954W	21			
	FL	Italy	2,860C→T	R954W	21		1	
	GA	USA-British	2,860C→T	R954W	21		13	
	GF	Egypt	2,860C→T	R954W	21			
	AV	USA-MEA	1,067T→C	M356T	8	Yes	26	
	FF	Turkey	2,839A→G	M947V	20		27	
	FS	Italy	none					
(c) Individuals with sporadic CFEOM1								
	G	USA	2,860C→T	R954W	21	Yes	14	
	J	Netherlands	2,860C→T	R954W	21			
	AS	USA	2,860C→T	R954W	21			
	AW	USA	2,860C→T	R954W	21	Yes	15	
	BA	USA	2,860C→T	R954W	21			
	BL	Venezuela	2,860C→T	R954W	21			
	DD	Germany	2,860C→T	R954W	21			
	FG	UK	2,860C→T	R954W	21	Yes	16	
	GK	Australia	2,860C→T	R954W	21	Yes	17	
	EZ	USA	2,861G→A	R954Q	21			
	JC	Italy	2,861G→A	R954Q	21	Yes	22	
	AL	USA	3,029T→C	I1010T	21	Yes	24	
	CA	USA	2,840T→G	M947R	20	Yes	28	
(d) Summary of <i>KIF21A</i> mutations in CFEOM1								
CFEOM1	Mutation frequency						With mutation	No mutation
	1,067T→C	2,839A→G	2,840T→G	2,860C→T	2,861G→A	3,029T→C		
Pedigrees	2/32 (6%)	1/32 (3%)	–	23/32 (72%)	4/32 (13%)	1/32 (3%)	31/32 (97%)	1/32 (3%)
Sporadic cases	–	–	1/13 (8%)	9/13 (69%)	2/13 (15%)	1/13 (8%)	13/13 (100%)	0/13 (0%)
Total combined	2/45 (4.5%)	1/45 (2%)	1/45 (2%)	32/45 (71%)	6/45 (13%)	2/45 (4.5%)	44/45 (98%)	1/45 (2%)
aa	M356T (4%)	M947V (4%)	M947R	R954W (84%)	R954Q	I1010T (4%)		

^aNumbering starts from the A of the initiation codon. ^bDAH, disease-associated haplotypes as defined by *de novo* mutations, polymorphisms and three new polymorphic markers within and adjacent to *KIF21A*. We assigned a number to each unique haplotype associated with each *KIF21A* mutation. Thus, each of the 1,067T→C and 3,029T→C mutations, and at least 17 of the 32 2,860C→T and 5 of the 6 2,861G→A mutations, are associated with unique disease-associated haplotypes and probably arose independently. aa, amino acid; FC, French Canadian. MEA, mixed European ancestry; nt, nucleotide.

Next, we identified 15 additional pedigrees and 13 sporadic cases that met our phenotypic criteria⁴ for CFEOM1, excluding two small pedigrees in whom CFEOM1 was not linked to *FEOM1* (ref. 4). Results of haplotype analysis of the 11 pedigrees with adequate enrollment were consistent with linkage to *FEOM1* (**Supplementary Fig. 1** online). We found that 13 pedigrees and 12 sporadic cases harbored one of the mutations identified in the initial screen. In addition, pedigree FF harbored a 2,839A→G nucleotide substitution (resulting in M947V), and individual CA with sporadic CFEOM1 harbored a 2,840T→G nucleotide substitution (resulting in M947R). These mutations are at nucleotide positions 1 and 2 of codon 947 (**Table 1b,c** and **Fig. 1c,d**).

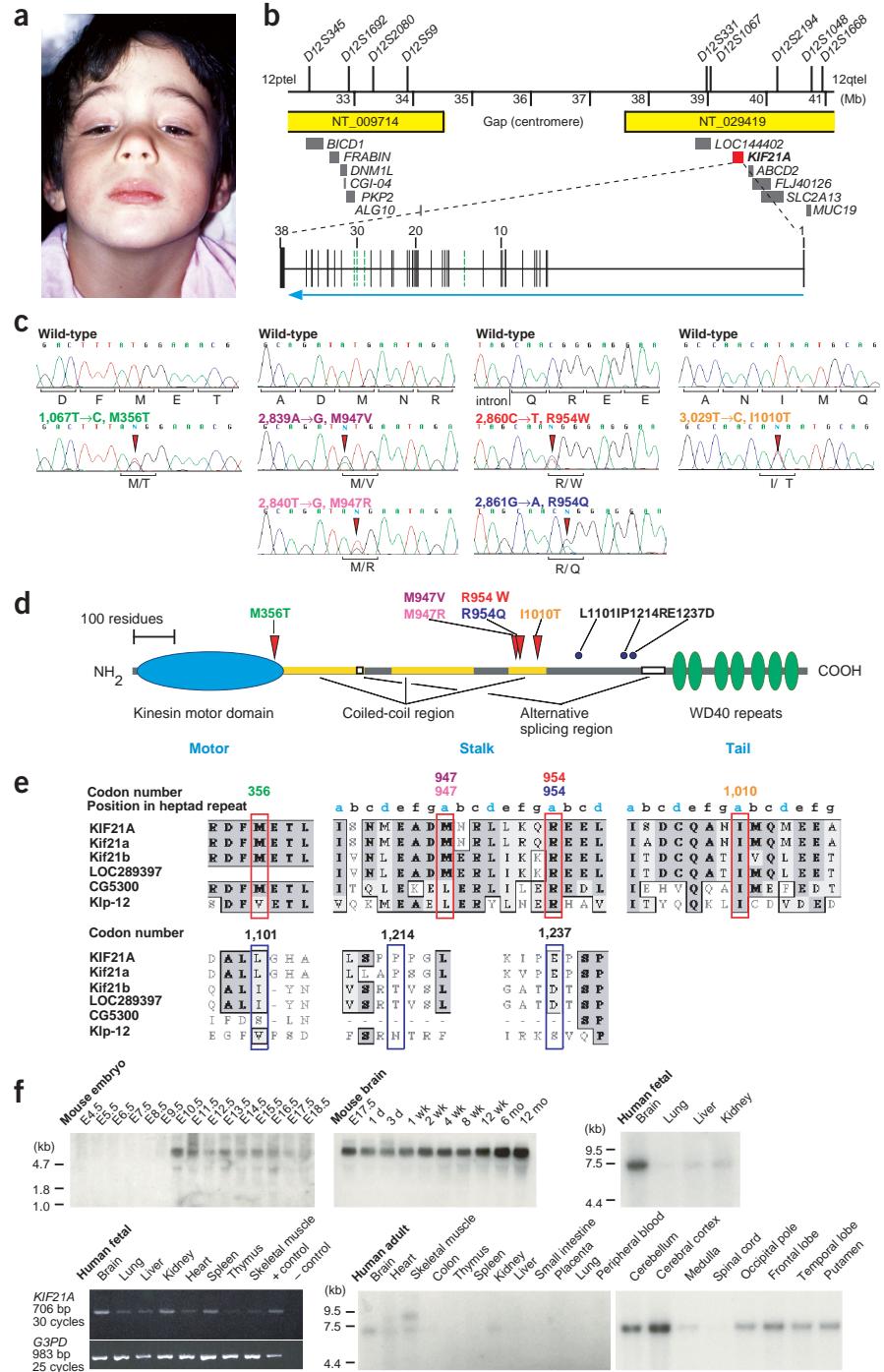
Affected individuals were heterozygous with respect to each mutation, and each mutation segregated with the disease phenotype and was not present on at least 210 control alleles from unrelated individuals of mixed ethnicity. To further establish the pathogenicity of the mutations, we identified 12 cases for which we had DNA samples from an apparent CFEOM1 founder individual and from both unaffected parents. In each case, the unaffected parents did not harbor the change, establishing these as *de novo* mutations (**Table 1**). Notably, haplotype analysis showed that the five *de novo* mutations that occurred in the autosomal dominant CFEOM1 pedigrees (**Table 1a,b**) arose exclusively on the paternal allele. The parental origin cannot be determined in individuals with sporadic *de novo* mutations causing CFEOM1. In addition, we detected 13 polymorphisms in *KIF21A* (**Fig. 1d,e** and **Supplementary Table 1** online).

In total, we identified *KIF21A* mutations in 98% of CFEOM1 probands; four of the six mutations are recurrent, and the two unique mutations alter the same amino acid (**Table 1d**). All six mutations alter nucleotides that are identical in mouse and human and amino acid residues that are highly conserved in *KIF21A* homologs (**Fig. 1e**). The independent nature of the recurrent mutations is supported by the ethnic and geographic diversity of the probands and by the occurrence of *de novo* mutations and multiple disease-associated haplotypes (**Table 1a–c**). We did not identify a mutation in pedigree FS, whose phenotype is consistent with linkage to both *FEOM1* and *FEOM3* (ref. 7,8; **Supplementary Fig. 1** online). This small pedigree confirms the genetic heterogeneity of CFEOM1 and, together with previous data⁴, suggests that mutations in *FEOM3* may be a rare cause of CFEOM1.

Northern-blot analysis and RT-PCR support a role for *KIF21A* in development (Fig. 1f). In mouse, *Kif21a* is first detected at embryonic day (E) 10.5, corresponding to approximately the fifth week of human gestation, when the oculomotor nerve and extraocular muscles are developing. In human fetal and adult tissues, we detected a 7.4-kb *KIF21A* transcript most abundantly in brain.

Kinesins and dyneins are molecular motors responsible for microtubule-dependent transport of cargo; in neurons, they are responsible for anterograde and retrograde axonal transport, respectively. *KIF21A*, *KIF21B* and *KIF4* comprise one of the ~14 classes of human kinesins⁹, and their predicted structures are similar to that of classical kinesin, with an N-terminal motor domain that interacts with the

Figure 1 Identification of the gene associated with CFEOM1. (a) A child with CFEOM1 who harbors the mutation 2,860C→T and has bilateral ptosis and bilateral infraducted (downward) eye position in primary gaze with a chin-up head posture. She cannot raise either eye above the midline. (b) Physical map of the *FEOM1* region flanked by *D12S345* and *D12S1668* (refs. 2–5). The horizontal line at the top of the figure represents the centromeric region of chromosome 12. Polymorphic markers are indicated above, and the physical distance (in Mb) and genomic sequence (in yellow with a gap at the centromere) are shown below the horizontal line. *KIF21A* is represented by a red box, and other known or putative genes are shown in gray. An expanded view of the *KIF21A* genomic structure is shown underneath, with the alternative splicing exons indicated as dashed green lines and the horizontal blue arrow indicating the direction of transcription. (c) *KIF21A* mutations in CFEOM1. Automated genomic sequence analysis of unaffected controls (top) and individuals with CFEOM1 (middle and bottom) showing each heterozygous mutation of *KIF21A*. The corresponding normal and mutated amino acid residues are indicated under each triplet codon. (d) Predicted *KIF21A* protein structure with the domains indicated. The motor domain is blue, coiled-coil regions of the stalk are yellow, alternatively spliced regions are white and the seven WD40 repeats in the tail are green. The location of amino acids altered by disease-causing mutations (red triangles) or non-pathogenic polymorphisms (blue dots) are indicated. M947V is the only disease-associated conservative amino acid change we identified. (e) Human *KIF21A* amino acid sequence and alignment with homologs surrounding each mutation (boxed in red above) and non-pathogenic amino acid alteration (boxed in blue below). For mutations in a coiled-coil region, positions a–g in each heptad are indicated. Identical amino acid residues are highlighted in dark gray; similar residues are highlighted in light gray. The predicted human *KIF21A* protein shares 93%, 60%, 53%, 39% and 35% identity with the mouse *Kif21a*, mouse *Kif21b*, rat *Kif21* (LOC289397), *D. melanogaster* CG5300 and *C. elegans* Klp-12 homologs, respectively. Rat *Kif21* sequence lacks its motor domain. The *KIF21A* mutations associated with CFEOM1 alter residues that are conserved among these homologs, whereas the non-pathogenic changes alter residues that are not conserved. (f) Expression analysis of *KIF21A* mRNA by northern-blot hybridization and RT-PCR. In mouse whole embryos, expression of *Kif21a* began at ~E10.5 and then slowly decreased. In mouse brain, *Kif21a* was expressed at all ages tested and expression increased gradually with age. In human fetal tissue, *KIF21A* mRNA was abundant in brain, with lower levels in liver and kidney. RT-PCR analysis of human fetal tissues showed a similar pattern, with *KIF21A* expressed most abundantly in brain followed by kidney and spleen, with lower levels in other tissues. In human adult tissue, a *KIF21A* transcript of ~7.4 kb was expressed primarily in brain with lower expression levels in heart, skeletal muscle and kidney. A second transcript of ~9.0 kb was detected in skeletal muscle; its function has not been determined. *KIF21A* was expressed abundantly in most of the central nervous system.



microtubule track, a central coiled-coil stalk and a C-terminal tail that interacts with the transported cargo. Mouse *Kif21a* was found to be enriched in adult neural tissues⁶. Notably, *Kif4* transports membranous organelles containing L1, a cell adhesion molecule important to axonal formation and extension in young neurons¹⁰.

Five of the six mutations in *KIF21A* associated with CFEOM1 alter only three amino acid residues, each located in position 'a' of a heptad (a–g) repeat in a coiled-coil region of the *KIF21A* stalk (Fig. 1d,e). The stalk is the site of kinesin dimerization, and the α -helical heptad coiled-coil regions are crucial for the association and stability of the dimeric structure, with the intertwined molecules touching at positions a and d. The location and recurrence of these *KIF21A* mutations suggest that they may have a dominant negative effect by interfering with the interaction between *KIF21A* and itself or its unidentified partners.

Only two disorders have been previously attributed to mutations in kinesin molecules, Charcot–Marie–Tooth disease type 2A¹¹ and hereditary spastic paraplegia (SPG10)¹². These disorders were reported in single pedigrees harboring mutations that altered invariant residues in the motor domain of *KIF1B β* and *KIF5A*, respectively, and were proposed to disrupt motor function, resulting in aberrant axonal trafficking primarily affecting the longest axons of the peripheral and central nervous system in a length dependent manner. Of the six mutations associated with CFEOM1 that we identified, only 1,067T→C maps to the *KIF21A* motor domain. We do not yet know if this mutation interferes directly with motor function.

CFEOM1 probably results from the inability of mutated *KIF21A* to successfully deliver a cargo essential to the development of the oculomotor axons, neuromuscular junction or extraocular muscles. Further studies of *KIF21A*, including the identification of its cargo and interacting proteins, should help elucidate why the oculomotor axis is selectively vulnerable to these mutations and lead to insights into the role of the kinesin stalk in health and disease.

GenBank accession numbers. *KIF21A* cDNA reference sequence, AY368076; *KIF21A* genomic sequence, AC084373, AC090668 and AC121334; *Kif21a*, NM_016705 and NP_057914; *Kif21b*, NP_064346; *Rattus norvegicus* *Kif21* protein (LOC289397), XP_223090; *Drosophila melanogaster* *Kif21* protein (CG5300), NP_609398; *Caenorhabditis elegans* *Klp-12* protein, BAB18763.

Note: Supplementary information is available on the Nature Genetics website.

ACKNOWLEDGMENTS

We thank all the participants in this study; J.H. Calhoun, R. Baker, E. Ballard, G. Rogers and R. Fellows for pedigree referrals; J. Scharf and A. Beggs for critically reading this manuscript; K. Miura and R.R. Bennett for advice and suggestions; M.P. Rogines-Velo-Sardi and C. Miranda for discussion; and C. St Hilaire for technical assistance. This work was supported by grants from the US National Institutes of Health and by the Children's Hospital Mental Retardation Research Center.

COMPETING INTERESTS STATEMENT

The authors declare that they have no competing financial interests.

Received 17 August; accepted 10 October 2003

Published online at <http://www.nature.com/naturegenetics/>

1. Engle, E.C. *et al.* *Ann. Neurol.* **41**, 314–325 (1997).
2. Engle, E.C., Kunkel, L.M., Specht, L.A. & Beggs, A.H. *Nat. Genet.* **7**, 69–73 (1994).
3. Engle, E.C. *et al.* *Am. J. Hum. Genet.* **57**, 1086–1094 (1995).
4. Engle, E.C. *et al.* *BMC Genet.* **3**, 3 (2002).
5. Uyama, E. *et al.* *Neuromuscul. Disord.* **13**, 472–478 (2003).
6. Marszalek, J.R., Weiner, J.A., Farlow, S.J., Chun, J. & Goldstein, L.S. *J. Cell. Biol.* **145**, 469–479 (1999).
7. Doherty, E. *et al.* *Invest. Ophthalmol. Vis. Sci.* **40**, 1687–1694 (1999).
8. Mackey, D.A. *et al.* *Hum. Genet.* **110**, 510–512 (2002).
9. Miki, H., Setou, M., Kaneshiro, K. & Hirokawa, N. *Proc. Natl. Acad. Sci. USA* **98**, 7004–7011 (2001).
10. Peretti, D., Peris, L., Rosso, S., Quiroga, S. & Caceres, A. *J. Cell. Biol.* **149**, 141–152 (2000).
11. Zhao, C. *et al.* *Cell* **105**, 587–597 (2001).
12. Reid, E. *et al.* *Am. J. Hum. Genet.* **71**, 1189–1194 (2002).
13. Magli, A., De Berardinis, T., D'Esposito, F. & Gagliardi, V. *BMC Ophthalmol.* **3**, 6 (2003).
14. Harley, R.D., Rodrigues, M.M. & Crawford, J.S. *J. Pediatr. Ophthalmol. Strabismus* **15**, 346–358 (1978).
15. Brodsky, M. *Ophthalmology* **105**, 717–725 (1998).